Direct determination of the electronic structure of S_4N_4 by x-ray and ultraviolet photoemission

W. R. Salaneck, J. W-p Lin, A. Paton, C. B. Duke, and G. P. Ceasar
Xerox Webster Research Laboratories, Webster, New York 14580
(Received 21 October 1975)

The results of a study of the electronic structure of S_4N_4 molecules are reported. The photoemission techniques employed include: x-ray photoemission spectroscopy (XPS) of the full valence band of thin films composed of S_4N_4 molecules; XPS core-level spectra of S_4N_4 molecules in the solid state as well as in the gas phase; and ultraviolet photoemission spectroscopy of the uppermost ionization potentials of S_4N_4 molecules in the gas phase. The data are analyzed using a self-consistent-field molecular-orbital calculation in the complete-neglect-of-differential-overlap approximation. Chemical shifts are observed in the S_4N_4 gas phase and solid-sample core-level spectra and are used to obtain an estimate of the amount of charge transfer $q \approx e/2$. A polarization energy 1.2 eV is deduced. The optical-absorption spectrum of S_4N_4, analyzed using a configuration-interaction treatment of our molecular orbitals, is found to be dominated by molecular excitons.

I. INTRODUCTION

The electronic structure of both solid and gaseous S_4N_4 has been a topic of interest for nearly two decades[1-9] because of the unusual atomic geometry of the S_4N_4 molecule,[10] itself. Specifically, unlike the situation in the compounds of phosphorous and arsenic with sulfur, in S_4N_4 the sulfur atoms are threefold coordinated whereas the nitrogens are twofold coordinated rather than vice versa.[11] This fact leads to the chemical reasoning that either a charge transfer of $q \sim e$ occurs from the sulfur to the nitrogen leading to two "lone-pair" electrons on each of the sulfurs and four on each of the nitrogens,[6] or that both the sulfur and nitrogen atoms contain two lone-pair electrons, and each contributes one additional electron to orbitals which are "delocalized" throughout the molecule.[1-4,8] Not only have these issues been left unresolved, but also more recently intensive interest[12-18] has arisen in the superconducting inorganic polymer $(SN)_x$ which exhibits an atomic geometry rather similar to that of S_4N_4 when the interactions between sulfur atoms on different (SN) chains are considered.[19] Consequently, spectroscopic measurements of the electronic structure of S_4N_4 and the interpretation of such measurements in terms of molecular-orbital models are of direct interest in establishing the origin of several unusual properties of sulfur-nitrogen compounds.

In this paper we report direct measurements in S_4N_4 of the electronic orbital eigenvalue spectrum by valence-electron photoemission and of the S-N charge transfer via the analysis of photoemission from the N(1s) and S(2p) core levels. From the latter, we infer a charge transfer from S to N of about $\frac{1}{2}e$ in S_4N_4 which suggests the delocalization of the higher-energy valence electrons in this material. We analyze the valence-electron photoemission via an extension of our earlier self-consistent field (SCF) molecular-orbital (MO) models for[20,21] sulfur- and[22] nitrogen-containing materials. While such an analysis does not respond directly to the localized-versus-delocalized-orbital issue as raised in the chemical literature[6-8] (because the molecular orbitals are delocalized by construction, being the molecular analogues of Bloch states in a solid), it does permit the detailed interpretation of the photoemission spectra. Specifically, our MO models employing the complete neglect of differential overlap (CNDO) approximation[23,24] yield a quantitative interpretation of high-resolution valence-electron photoelectron spectra and a quantitative prediction of the uv absorption spectrum of S_4N_4. Therefore some confidence can be placed in our CNDO-S assignments of the eigenvalues and characteristics of the various molecular orbitals of S_4N_4.

The presentation of our results is divided into four parts. First, in Sec. II we present a discussion of our experimental studies leading to (a) x-ray photoemission (XPS) spectra of the valence electrons of S_4N_4 molecules in solid thin films and of the N(1s) and S(2p) core levels of S_4N_4 in both the solid and the gas phase, and (b) uv photoemission (UPS) spectra of S_4N_4 molecules in the gas phase. The UPS gas-phase data provide the highest available resolution for studying the smaller valence-electron ionization potentials. The XPS data yield both a measure of the entire valence band and information about the local electronic environment of individual sulfur and nitrogen atoms through a chemical shift analysis of S_8, S_4N_4, and N_2 molecules. In Sec. III, we describe the construction of our "CNDO-S" molecular-orbital model, where we use an "S" to indicate "spectroscopic parameterization". In Sec. IV, the CNDO-S MO densities of states, $\rho_c(E)$ are compared with the XPS and UPS spectra, and the first few singlet optical transitions are calculated from the CNDO-S MO's using a configuration interac-

tion procedure in order to account for relaxation and Coulomb effects that dominate the optical spectra of small molecules. Also, in this section certain conclusions are drawn from our study that bear on the understanding of the electrical properties of $(SN)_x$. The application of our CNDO-S model to describe the orbital eigenvalue spectra of SN and S_2N_2 is presented in the Appendix.

II. EXPERIMENTAL RESULTS

S_4N_4 was prepared following a modification of the procedure of Goehring.[25,26] The yellow solid was extracted with freshly distilled anhydrous *p*-dioxane and freeze dried. Further purification of S_4N_4 was carried out by multiple recrystallizations from hot benzene. ir spectra[27] and melting-point determinations (melting point, 185.5–186.5 °C) indicated that the material was extremely pure. Chemical analysis of the S_4N_4 yielded an elemental content of 69.80% S and 30.10% N versus calculated values of 69.60% and 30.40%, respectively.

The valence electron and core-level XPS spectra were recorded on an AEI ES 200B photoelectron spectrometer utilizing Mg $K\alpha$ radiation, for which $h\nu = 1253.7$ eV and $\Delta(h\nu) \approx \frac{3}{4}$ eV. The data were recorded using multiple scanning techniques incorporating a Nicolet 1072 multichannel analyzer. Facilities for simultaneous vapor deposition and data acquisition were incorporated into the spectrometer. The conditions for the vapor deposition of S_4N_4 molecules without thermal decomposition were determined through temperature studies of the XPS core-level spectra, and UPS gas-phase data. It was found that up to 80 °C, no significant thermal decomposition of the S_4N_4 molecules occurred. Therefore we prepared thin films of S_4N_4 molecules by packing a quartz capillary tube with powdered S_4N_4, and subliming the material by holding the quartz capillary tube at 80 °C in a vacuum of $P \lesssim 10^{-9}$ Torr. The pressure rose to $p \lesssim 10^{-8}$ Torr during vapor deposition. Sputter cleaned pure gold foils maintained at $T < -30$ °C were used for the substrates.

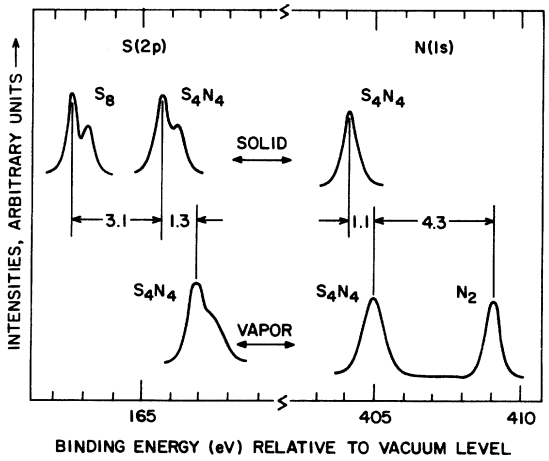

FIG. 1. X-ray photoemission core-level data of S_4N_4 are shown as taken under two different conditions. The upper curves show the chemical shift of the S(2*p*) levels relative to those in S_8, both obtained from thin film samples prepared by vapor deposition onto gold foils in the vacuum chamber of the spectrometer. The lower curves illustrate the chemical shift of the $N(1s)$ level in S_4N_4 relative to that in N_2 obtained in simultaneously the vapor phase. The S_8 and N_2 molecules are convenient reference molecules, since the effective charges on the sulfur and nitrogen atoms in these molecules are zero.

Under the conditions prescribed above, thin films of S_4N_4 had S(2*p*)/N(1*s*) counts ratios of unity. These core-level counts ratios were obtained using the fixed-analyzer-transmission mode of energy scanning such that the sensitivity to all elements was equal. Cross-section values were taken from Hartree-Fock calculations by Scofield.[28] The proper S/N counts ratios are unlikely to occur if thermal decomposition occurs during vapor deposition, since some of the decomposition products are gaseous at the −30 °C substrate temperature.[29] In addition, the XPS core-level spectra of S_4N_4 in the gas phase at +80 °C also indicated a S/N counts ratio of unity and single S(2*p*) and N(1*s*) lines, confirming the XPS measurements in the solid phase. The core-level spectra are shown in Fig. 1, and the XPS valence-electron spectra in Fig. 2.

The energy calibration and film thickness control of the solid S_4N_4 samples was achieved by observing, e.g., the S(2*p*) core-level spectrum during vapor deposition, at rates of about ~1 Å/min. For samples sufficiently thin that the substrate Au (4*f*) levels could still be observed, the S(2*p*) energies can be referenced to the Au($4f_{7/2}$) line at 83.8 eV.[30] Vapor deposition was continued until the Au(4*f*) lines could no longer be observed, and then either terminated or continued at ~0.1 Å/min to maintain a fresh surface. Subsequent observation of the reference core levels indicated that no sample charging occurred in these thin films. Final thickness of the S_4N_4 films were estimated to be < 100 Å. At the end of an all-day run, the C(1*s*) signal was negligible and that due to O(1*s*) was not detectable.

The XPS vapor-phase data were acquired using the standard AEI gas cell with an aluminum-coated Melinex (polycarbonate) window. Cell pressures of only $p \sim 10^{-2}$ Torr were achieved, however, when the S_4N_4 source and the gas cell housing were maintained at +80 °C. At these low pressures, statistics on the valence band were poor and consequently only the gas-phase core-level spectra

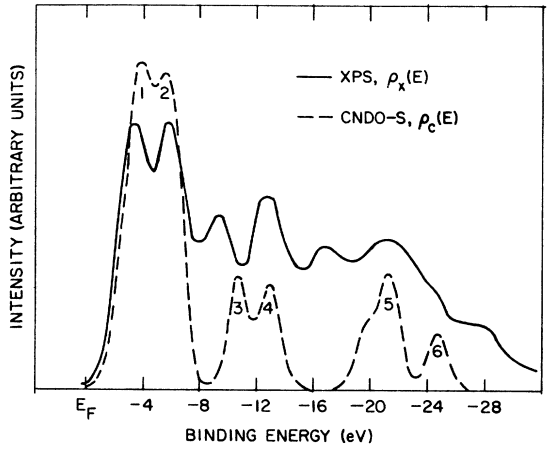

FIG. 2. X-ray valence-electron photoemission spectra of S_4N_4 molecules, obtained from thin film samples prepared by vapor deposition in the vacuum chamber of the spectrometer, are shown as a solid curve $\rho_x(E)$. The calculated valence-electron density of states $\rho_c(E)$, obtained by representing each orbital eigenvalue by a Gaussian width 1 eV, is shown as a dashed line. The slight nonalignment of the peaks in the two curves is attributed to the nonlinearity of relaxation effects (deviations from Koopman's theorem) across the valence-band region. The peaks are numbered for reference to Table IV.

are presented. Nitrogen gas was introduced for calibration. The chemical shift of the nitrogen in S_4N_4 relative to N_2 in the gas phase is displayed in Fig. 1. Because of the geometry of the experiment, core-level energies of molecules in the vapor phase are referenced to the vacuum level.[31] The corresponding shift of the S(2p), obtained relative to S_8 in the solid phase,[21] also is shown in Fig. 1.

The core-level energies of the solid film can be referenced to the vacuum level by observing the low-energy cutoff of the true secondary electron spectrum as discussed by, for example, Evans.[32] Since the electron analyzer was operated by maintaining 65 V across the hemispheres and sweeping the retarding potential, it is necessary to bias the sample substrate away from zero potential (ground) by at least 65 V. A common B battery of nominally 90 V was used with an accurate voltage determination accomplished by observing the amount of shift of the S(2p) or N(1s) levels. Then the difference between the low-energy cutoff V_c and the bias voltage V_0 is equal to the difference between the spectrometer effective work function and the work function of the sample thin film with its Fermi level coincident with that of the gold substrate,[32] $\Delta\phi = V_0 - V_c$. In four determinations, we find that $\Delta\phi = 2.9 \pm 0.1$ eV.

The UPS gas-phase spectra were recorded using the HeI lamp on a Vacuum Generators ESCA-2 photoelectron spectrometer operating at 30-meV resolution. Argon gas was used for calibration. The S_4N_4 was volatile enough to provide spectra at room temperature. In addition, spectra obtained at 80 °C were identical to those obtained at room temperature. These results, when taken together with those of the XPS core-level studies, indicate that no thermal decomposition of S_4N_4 molecules occurs up to +80 °C. The UPS gas-phase spectra obtained at +80 °C are shown in Fig. 3.

III. MODEL CALCULATIONS

Our objective in the analysis of the photoemission spectra described in Sec. II is the construc-

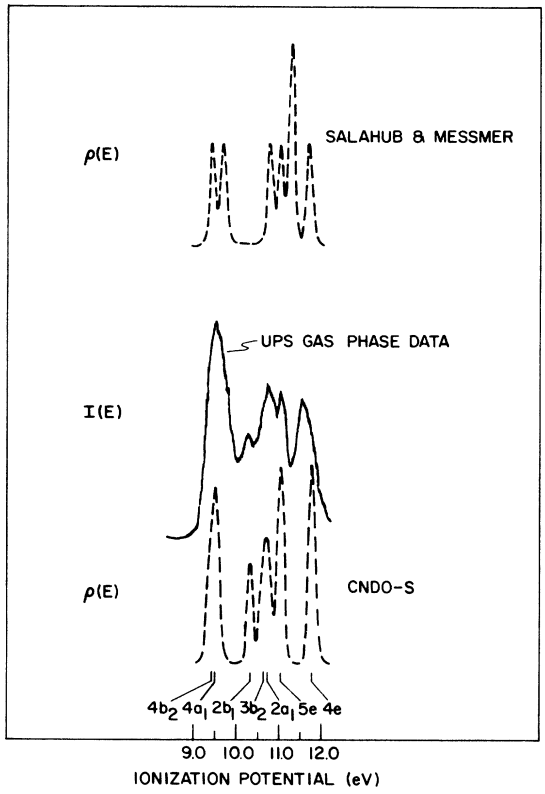

FIG. 3. Ultraviolet photoemission spectra of S_4N_4 in the gas phase at +80 °C is shown along with the valence-electron density of states obtained from CNDO-S MO eigenvalues that pertain to this energy region. The transitions are labeled by the irreducible representations of the point group of the S_4N_4 molecules D_{2d}. Data obtained at room temperature are generally indentical with those shown, but exhibit some decrease in intensity. The lower dashed curve represents the density of states calculated from our CNDO-S MO's using Gaussians of width 0.1 eV. The upper dashed curve is derived from the $X\alpha$ calculation of Salahub and Messmer (Ref. 9) in the same manner. Our calculated curve is shifted by −1.1 eV to line up the peaks in the first ionization potential. The curve corresponding to Salahub and Messmer's MO calculation was shifted by +3.2 eV.

tion of a single "spectroscopic" CNDO-S model which describes photoemission, optical-absorption, and resonance data simultaneously.[20–22,33] To accomplish this end, we utilize a standard[23] CNDO model, but adjust the off-diagonal matrix elements in order to describe the UPS photoemission spectra rather than Hartree-Fock calculations. The XPS and uv absorption spectra are, therefore, *predictions* rather than inputs of our parametrization. This section is devoted to a brief description of the model obtained by this procedure.

The CNDO model is defined by approximating the Hartree-Fock matrix, constructed in a basis of atomic orbitals, by[23,33]

$$F_{\mu\mu} = U_{\mu\mu} + (P_{AA} - \tfrac{1}{2}P_{\mu\mu})\gamma_{AA} + \sum_{B\neq A}(P_{BB} - Z_B)\gamma_{AB}, \tag{1a}$$

$$F_{\mu\nu} = H_{\mu\nu} - \tfrac{1}{2}P_{\mu\nu}\gamma_{AB}, \quad \mu \neq \nu, \tag{1b}$$

if the penetration integrals are neglected. The $P_{\mu\nu}$ are the density matrices in a basis defined by atomic orbitals labeled by μ. The subscripts A and B designate specific atoms in the molecule and indicate summation over all orbitals on that atom. The γ_{AA} are average single-center Coulomb integrals and γ_{AB} are the corresponding two-center integrals. The $U_{\mu\mu}$ are the one-electron core Hamiltonian matrix elements involving only the ion-core potentials associated with the orbital μ. We use for these quantities the expression[23]

$$U_{\mu\mu} = I_\mu - (Z_A - 1)\gamma_{AA}, \tag{2}$$

in which I_μ is the ionization potential for the orbital labeled by μ on the atom labeled by A whose net nuclear-plus-core-electron charge is Z_A.

The off-diagonal matrix elements of the one-electron Hamiltonian are given by the Wolfsberg-Helmholz formula[34]

$$H_{\mu\nu} = \tfrac{1}{2}K(I_\mu + I_\nu)S_{\mu\nu}, \tag{3}$$

in which we use different values of K for the s as opposed to the p and d atomic orbitals. The ionization potentials I_μ and intra-atomic Coulomb integrals γ_{AA} are taken from Sichel and Whitehead[35] and from Dewar and Lo[36] for sulfur and nitrogen, respectively. The interatomic two-center Coulomb integrals are obtained using the interpolation formula of Clark[37]

$$\gamma_{AB} = 14.397\ \text{eV}\left[\left(\frac{28.794\ (\text{Å/eV})}{\gamma_{AA}+\gamma_{BB}}\right)^2 + r_{AB}^2\ (\text{Å})\right]^{-1/2}. \tag{4}$$

Finally, the uv absorption spectra were calculated using a configuration interaction (CI) program based on an analysis like that given by Lowitz.[38] The charge densities in the CNDO-S ground-state calculations were taken to be self-consistent to within one part in 10^3. The resulting orbital eigenfunctions and eigenvalues were used as inputs to the CI analyses.

A synopsis of the parameters utilized in our final model, to which we shall refer as CNDO-S, is presented in Table I. The values of the Wolfsberg-Helmholtz parameter K_i were held fixed at their values[21] originally used for S_8. Thus, only the Slater exponents were varied in constructing off-diagonal one-electron matrix elements, Eq. (3), which lead to eigenvalue spectra in correspondence with the UPS spectra. The rationale for this procedure is described in detail by Lipari and Duke.[33]

Finally, we wish to emphasize that the orbital eigenfunctions obtained by a SCF calculation such as ours are delocalized orbitals, analogous to Bloch states in a periodic solid. These eigenfunctions diagonalize the Fock operator, Eqs. (1), and their associated eigenvalues (the energies of the individual MO's) correspond to ionization potentials.[20–24,33,39,40] Since relaxation effects are thought to be roughly constant for valence electrons, the one-electron energies are expected to be good approximations to the valence-band photoemission energies to within an over-all additive constant[40] (Koopman's theorem). On the other hand, the localized bond orbitals (the analogues of Wannier orbitals in solids) such as sp^3, etc., may be related to the delocalized orbitals through a unitary transformation which leaves observables such as the total energy and the total charge distribution unchanged. In the basis of the localized bond orbitals, however, the energy operator is *not* diagonal, and thus energies associated with localized orbitals are not observables in a photo-

TABLE I. Parameters used in the CNDO-S model of the electronic structure of S_4N_4. The Wolfsberg-Helmholtz parameters are $K_s = 0.5$ and $K_p = K_d = 0.7$.

Atom	I_s (eV)	I_p (eV)	I_d (eV)	γ_{AA} (eV)	ζ_s (Å^{-1})	ζ_p (Å^{-1})	ζ_d (Å^{-1})
S	20.8	12.0	2.0	9.2	3.21	4.16	2.87
N	27.5	14.3	···	12.4	4.63	4.35	···

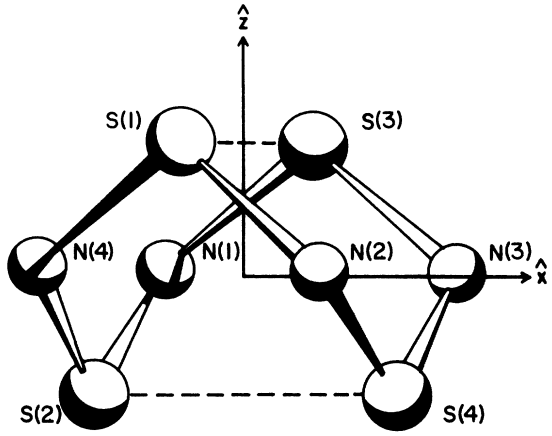

FIG. 4. Geometry of the S_4N_4 molecule is shown in perspective (Ref. 10).

emission experiment. Optical transitions must also be calculated from the eigenstates (delocalized orbitals) for the same reason.

IV. RESULTS

A. Valence-electron photoemission

As noted above, the input data for the construction of our spectroscopic CNDO-S model are the UPS gas-phase spectra shown in Fig. 3 and the known[10] atomic geometry of S_4N_4 as specified in Fig. 4 and Table II. The direct output of the adjustment of the off-diagonal one-electron matrix elements [Eq. (3) by virtue of variations in the ξ_i] is the CNDO-S density of states illustrated in the lower panel of Fig. 3. In the upper panel of Fig. 3, a comparable valence-electron density-of-states calculated from the self-consistent-field–$X\alpha$–scattered-wave (SCF-$X\alpha$-SW) eigenvalue spectrum of Salahub and Messmer[9] is presented for comparison.

The low-resolution density of states suitable for comparison with the XPS valence-electron spectrum is a prediction of our model. It is compared with the XPS spectrum, $\rho_x(E)$ in Fig. 2. The low-resolution density-of-states function $\rho_x(E)$ is constructed from the orbital eigenvalue spectrum (given in Table III) by replacing the eigenvalue of each occupied orbital with a Gaussian of 1 eV width to simulate instrumental resolution and solid-state effects, then summing over them. Utilizing our CNDO-S model, all of the weak structure in the lower valence-band region (i. e., higher binding energies) is accounted for. In S_8 molecules, the lower valence band originates from S(3s)-derived MO's, whose spatial characteristics and energy spacing correspond to ring quantized orbitals,[41] with zero, two, four, six, and then eight nodes in order of decreasing binding energy. In S_4N_4 the lower valence band also corresponds to ring-quantized orbitals derived from S(3s) and N(2s) atomic orbitals, well separated in energy from the upper valence band (lower binding energy), which is derived primarily from the S(3p) and N(2p) atomic orbitals. The atomic origin of the structural features in $\rho_x(E)$ are tabulated in Table IV.

From the chemical perspective, sulfur in S_4N_4 corresponds to sp^3 hybridization.[42] The N-S-N bond angle[10] is about 105°, and thus a small amount of S(3d) mixing is necessary to completely account for the geometry. The S(3d) contributions to the MO's are shown in Table IV. The photoemission spectrum, however, contains contributions from MO's derived from the S(3s) and N(2s) atomic orbitals in a *different* energy range than the contributions from the MO's derived from the S(3p) and N(2p) atomic orbitals. No inconsistency exists between the two preceding sentences because the localized bond orbital (LBO) basis functions, such as sp^3, sp^2, and sp, do not diagonalize the energy operator.[39] The LBO basis is related to the MO (energy eigenfunction) basis through a unitary transformation that leaves the total energy and the total charge distribution unchanged. "Orbital energies" associated with LBO functions do not correspond, therefore, to ionization potentials. Consequently, the atomic geometry is not simply related to the structure in the photoemission spectrum.

The use of the (most-widely accepted) concept of s-p hybridization, noted in the preceding paragraph, should not be confused with an alternate "spectroscopic" usage of the term hybridization. For example, Gopinathan and Whitehead[8] (GW) have studied S_4N_4 using a "CNDO-BW" model appropriate for average ground-state geometry problems.[43] The Gopinathan-Whitehead concept of the "lack of s-p hybridization" is equivalent

TABLE II. Atomic coordinates for S_4N_4 based upon the structure determination by Sharma and Donohue (Ref. 10). The numerical values are $\alpha = 1.225\,000\,0$ Å, $\beta = 0.989\,984\,9$ Å, and $\gamma = 1.277\,187\,5$ Å. The accuracy indicated is merely for convenience in deducing the symmetries of the MO wave functions output by our computer program.

Atom	x	y	z
S(1)	0	$-\alpha$	β
S(2)	$-\alpha$	0	$-\beta$
S(3)	0	α	β
S(4)	α	0	$-\beta$
N(1)	$-\gamma$	γ	0
N(2)	γ	$-\gamma$	0
N(3)	γ	γ	0
N(4)	$-\gamma$	$-\gamma$	0

TABLE III. First 28 MO's and the corresponding energy eigenvalues of S_4N_4. The energies have been adjusted by 1.07 eV so the energy of the highest occupied molecular orbital is coincident with the first ionization potential of Fig. 3. The MO's are labeled by the irreducible representations of the point group of the S_4N_4 molecule D_{2d}. The relative S(3s), S(3p), N(2s), and N(2p) origin of each MO is indicated to the nearest percent.

Orbital	Symmetry	E (eV)	%S(3s)	%S(3p)	%S(3d)	%N(2s)	%N(2p)
Virtual							
32	$3a_2$	−0.13	0	44	3	0	52
30,31	$8e$	−0.52	3	39	4	0	54
29	$5b_2$	−0.57	7	36	2	0	56
28	$5a_1$	−1.07	2	31	2	3	63
26,27	$7e$	−1.23	3	37	2	3	55
25	$3b_1$	−1.70	0	42	4	2	52
23,24	$6e$	−4.51	1	81	0	0	17
Occupied							
22	$4b_2$	−10.54	1	68	2	0	29
21	$4a_1$	−10.56	0	91	0	2	6
20	$2b_1$	−11.41	0	52	1	3	44
19	$3b_2$	−11.72	1	57	2	0	40
18	$2a_2$	−11.85	0	3	2	0	95
16,17	$5e$	−12.12	0	46	1	1	52
14,15	$4e$	−12.87	4	57	1	1	38
12,13	$3e$	−13.62	0	30	3	2	65
11	$3a_1$	−13.86	6	71	1	0	22
10	$1a_2$	−13.97	0	52	0	0	48
9	$2b_2$	−14.39	0	38	2	0	60
7,8	$2e$	−18.66	73	4	0	14	9
6	$2a_1$	−20.64	46	4	2	43	5
5	$1b_2$	−21.16	90	1	1	0	8
4	$1b_1$	−27.63	0	6	3	91	0
2,3	$1e$	−29.26	16	4	3	77	0
1	$1a_1$	−32.69	45	3	0	51	1

to our statement that the atomic-s and atomic-p orbitals contribute to the photoemission in different energy regions. A similar "definition" of hybridization enjoys common use in the literature on the bonding characteristics of the chalogens.[44]

B. Ultraviolet absorption

From the orbital eigenvalues displayed in Table III, the one-electron band gap, corresponding to the difference in energy between the highest occupied molecular orbital level and the lowest unoccupied molecular-orbital level, is about 6 eV. This is *not* the energy of the first optical transition, because of the failure of the independent-electron model of particle-hole excitations in small molecules.[20–22,33] Specifically, two physical phenomena conspire to invalidate the independent-particle model of optically-induced transitions in small molecules. First, the Coulomb matrix elements in the particle-hole state differ from those in the ground state. These differences create the binding energy of tightly-bound "Frenkel" excitons in conventional solid-state-physics nomenclature.[45] In addition, however, the eigenstates of the particle-hole system are linear combinations of the individual Hartree-Fock independent particle-hole states. A description of this phenomenon leads to the weakly bound "Wannier" excitons[45] in semiconductors. Without an explicit treatment of *both* aspects of the Coulomb inter-

TABLE IV. Atomic origin of the peaks in the XPS valence-band spectrum $\rho_x(E)$. The peaks are numbered in Fig. 2. The relative atomic orbital contribution is obtained by squaring the appropriate atomic orbital coefficient in the molecular orbital and summing over all molecular orbitals whose energies contribute to a given peak in $\rho_x(E)$.

	Relative percentages				
Peak No.	S(3s)	S(3p)	S(3d)	N(2s)	N(2p)
1	1	53	1	1	44
2	1	48	1	1	49
3	73	4	0	14	9
4	68	2	1	22	8
5	8	5	4	83	0
6	45	3	0	51	1

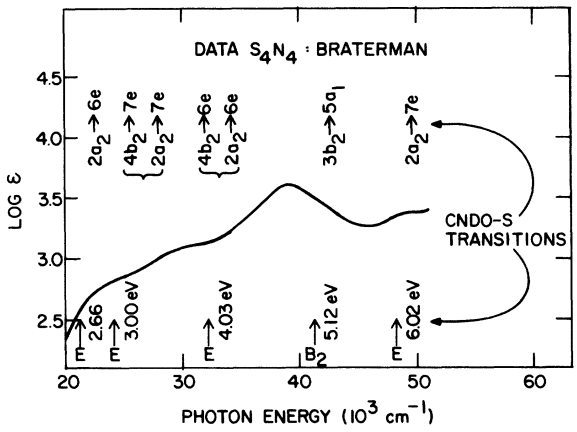

FIG. 5. Data of Braterman (Ref. 3) on the optical absorption of S_4N_4 molecules in solution is shown as a solid line. The optical transitions obtained by a configuration interaction treatment of the CNDO-S MO eigenvalues are shown as vertical arrows. The calculated transition symmetries also are indicated. B_2 corresponds to optical transitions polarized along the z axis of the molecule (see Fig. 4), while E corresponds to transitions polarized in the x-y plane. The dominant character of each transition is indicated across the top of the figure. Refer to Fig. 7 for the corresponding wave functions and an explanation of the notation.

action in molecules, however, the optical-absorption spectrum cannot be obtained from a MO calculation which also describes to the photoemission spectra.[21-22,33]

The CI procedure described in Sec. III takes into account the proper spinor character of the optical transitions (i. e., singlet and triplet) and determines the linear combinations of ground-state and excited-state wave functions that minimize the optical transition energies.[38] The first few singlet optical transitions in S_4N_4 are shown in Fig. 5, along with the data of Braterman[3] taken on S_4N_4 molecules in solution. Seven initially occupied and six initially unoccupied orbitals were used in the CI manifold. The absorption energies are in good agreement with the structural features in the $\log_{10}\epsilon$-versus-frequency (cm^{-1}) curve. Since we deal with Slater orbitals, however, our oscillator strengths are only an indication of negligible versus significant probability of the occurrence of an optical transition. The transitions indicated in Fig. 5 are the CI transitions having finite (nonzero) oscillator strengths based upon Slater orbitals, with the transition at 5. 12 eV having the largest oscillator strength of those shown. This strong peak around 5 eV was attributed by Braterman[3] to a transition from the S-S bonding highest occupied MO to S-S antibonding lowest unoccupied MO, $4b_2 \rightarrow 6e$ in Fig. 7. Our analysis, however, reveals that the $4b_2 \rightarrow 6e$ transition contributes mainly to the lower-energy structure near 4 eV. The 5-eV peak corresponds to a B_2 symmetry transition, which can only come from one degenerate state (e) to another *or* involve an a_1 state in D_{2d}.

C. Core-electron photoemission

The core-level spectra, shown in Fig. 1, can be used to obtain a measure of the charge transfer that occurs when S_4N_4 is formed from sulfur and nitrogen atoms. Solid films of S_4N_4 were prepared in precisely the same manner, and under the same conditions as the S_8 films previously studied.[21] Using the $S(2p_{3/2})$ line in S_8 molecules as the fiducial point, the sulfur atoms in S_4N_4 experience a chemical shift of 3.1 ± 0.1 eV. Using the N(1s) line in N_2 vapor as the fiducial point, the chemical shift of the nitrogen atoms in S_4N_4 vapor is -4.3 ± 0.3 eV. The absolute binding energies in the vapor versus in the solid are, of course, different due to the energy associated with the polarization of the solid by the hole in the final state, i. e., the so-called polarization energy.[31] Siegbahn and coworkers[46] have studied and tabulated the chemical shifts of sulfur and nitrogen atoms in a wide range of sulfur- and nitrogen-containing molecules. The N(1s) level shows a larger change in binding energy per unit effective charge than the $S(2p_{3/2})$ level, consistent with the difference in the chemical shift of the $S(2p_{3/2})$ with respect to that of the N(1s). From Siegbahn's tabulations, we find that both the chemical shift of the N(1s) and the $S(2p_{3/2})$ levels in S_4N_4 correspond to an effective charge of about 0. 6 of an electron. Our CNDO-S model predicts effective charges of 0. 47 electron, in fair agreement with the value inferred from the core-level shifts.

Using the biasing technique[32] discussed in Sec. II, the energy of cutoff of the secondary electrons was measured in order to obtain $\Delta\phi = V_0 - V_c$, the difference between the work function of the sample and the effective work function of the spectrometer. The core-level energies obtained on solid films can then be referenced to the vacuum level. This procedure enables an absolute comparison between the core-level energies obtained from molecules in the gas phase and from the same molecules in the solid state. We find that the shift in binding energy of the $S(2p_{3/2})$ in going from the vapor into the solid corresponds to -1.3 ± 0.2 eV, and the N(1s) corresponds to -1.1 ± 0.2 eV. Since relaxation effects are conceivably different for the N(1s) level than the $S(2p_{3/2})$, the agreement is quite remarkable. The error bars reflect the sample-to-sample variations, the accuracy within one sample being ± 0.1 eV. Thus, the so-called "polarization energy" of the solid S_4N_4 can be taken to be 1.2 ± 0.2 eV.

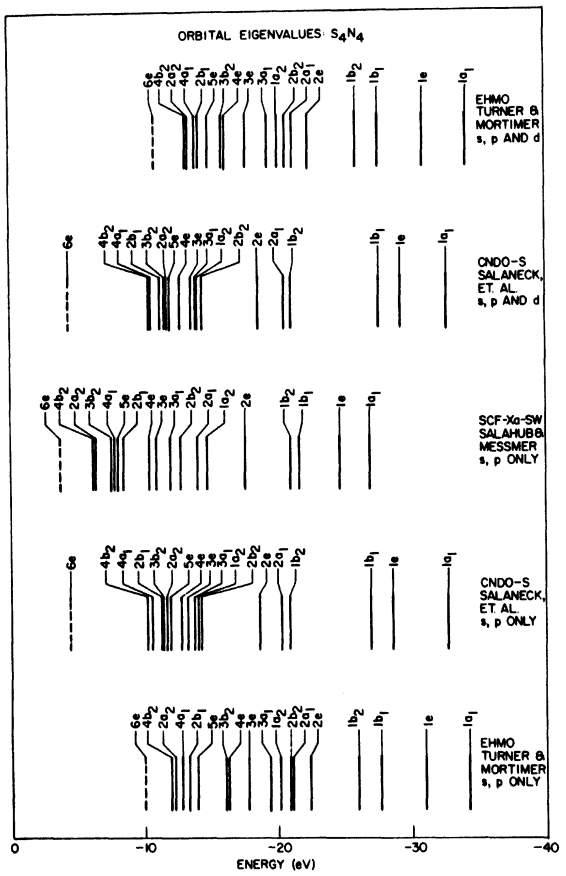

FIG. 6. Diagrammatic indication of the published orbital eigenvalue spectra of S_4N_4. The calculations labeled Extended-Hückel molecular orbital (EHMO) are those of Turner and Mortimer (Ref. 4). Those labeled SCF-$X\alpha$-SW were reported by Salahub and Messmer (Ref. 9). The eigenvalues labeled CNDO-S: *s*, *p*, and *d* are predicted by our CNDO-S model, whereas those labeled CNDO-S model in which the sulfur *d* electrons have been artifically removed from the basis set.

D. Previous studies of electronic structure of S_4N_4

The electronic structure of S_4N_4 molecules has been studied before by parametrizing MO calculations on average ground-state properties of the molecule. One of the earliest studies was by Lindqvist[1] who first discussed the possibility of S-S interactions occurring across the plane of the nitrogen atoms. The next analysis was that of Chapman and Waddinton,[2] who devised a phenomenological "electron-on-a-sphere" model to describe the strong uv absorption line near 5 eV in S_4N_4. Empirical (i. e., not self-consistent) molecular-orbital analyses of the optical spectra and geometrical shape of S_4N_4 were presented subsequently by Braterman,[3] by Turner and Mortimer,[4] and by Gleiter.[6] Most recently, self-consistent calculations have been reported using CNDO-2,[7] CNDO-BW,[8] and the SCF-$X\alpha$-SW[9] methods. Turner and Mortimer[4] as well as Salahub and Messmer[9] actually display their eigenvalue spectra, hence their results are compared with ours in Fig. 6. Moreover, the SCF-$X\alpha$-SW model results in a sufficiently good description of the UPS spectrum that the associated density of states is plotted in Fig. 3 together with our data and the CNDO-S density of states. The SCF-$X\alpha$-SW method also predicts a charge transfer from sulfur to nitrogen of 0.55*e*, in quite adequate agreement with the experimental value of 0.6*e* and the CNDO-S value of 0.47*e*.

From a comparison of our results with these earlier ones, two points emerge. First, the CNDO-S model is the first to provide a quantitative description of all the spectroscopic data (i. e, UPS, XPS, and uv absorption), and it is consistent with our earlier models of S_8,[21] As_4S_4,[20] and As_4Se_4.[20] Second, for a given CNDO model parametrization, the inclusion of the *d*-electron orbitals on the sulfur atoms evidently makes a modest but significant change in the eigenvalue spectrum as measured by comparison of the calculated density of states with the UPS spectrum.

E. S_4N_4 wave functions and implications for $(SN)_x$

Since the nature of the chemical bonding is reflected in a spectroscopic model by the characteristics of the eigenvalues, we display in Fig. 7 a schematic indication of the lower unoccupied and upper occupied orbitals (i. e., the "frontier" orbitals) in S_4N_4. In this section, we discuss some of the consequences of these orbitals, and their analogues in SN and S_2N_2 which are presented in the Appendix.

Perhaps the most significant feature of the frontier orbitals is the effect of the weak S-S interaction on the wave functions and the corresponding orbital energies. The weak S-S ($4b_2$) bonding orbital has the lowest ionization potential of any filled orbital. In particular, this highest occupied MO contains almost 70% of its charge density in the S-S bonding portion of the wave function. The lowest unoccupied MO, on the other hand, contains over 80% of its charge density in the corresponding S-S antibonding portion of the wave function. Thus, one might expect the uv absorption spectrum to be dominated by the transition between these two orbitals,[3] which does *not* turn out to be the case when configuration interaction is allowed as may be seen from Fig. 5. Another important issue, however, is the role of the S-S interactions on the conduction band states of $(SN)_x$.[19] The relative importance of the S-S and S-N interactions, of course, goes to zero as the S-S distance is made arbitrarily larger. For modest S-S spacings, therefore, the S-S inter-

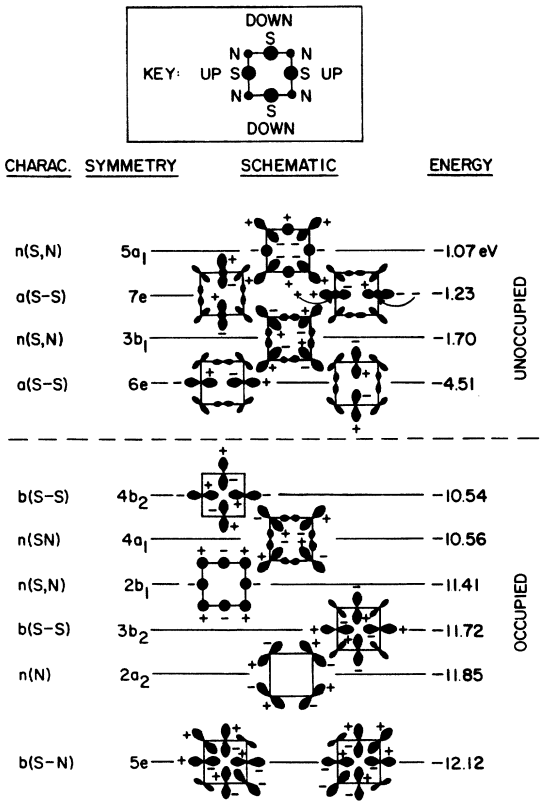

FIG. 7. Molecular orbitals corresponding to the upper-most seven occupied and the lower-most six unoccupied eigenstates are shown schematically. Refer to the insert for the geometry. The sulfur atoms occur in pairs above and below the plane of the four nitrogen atoms (see Fig. 4). The predominant character of each MO is indicated by the following notation: *b*, binding; *n*, nonbonding; *a*, antibonding; S, sulfur; N, nitrogen. For example *b*(S-N) indicates a sulfur-nitrogen bonding MO and *a*(S-S) indicates a sulfur-sulfur antibonding MO.

action affects significantly the MO's out of which the conduction band and the valence band would be built in a band structure model. In $(SN)_x$ crystals, where a weak S-S *inter*chain interaction is believed to occur,[47] the corresponding contributions of the S-S interaction are likely to become of comparable importance to those in S_4N_4.

The second point to note about the frontier molecular orbitals is that without the S-S across-the-ring interaction, these orbitals correspond approximately to a series of ring-quantized orbitals,[41] as discussed in an idealized case for S_4N_4 by Gleiter.[6] The vertical alternation of sulfur and nitrogen atoms normal to the plane of the ring results in a splitting of an otherwise (e.g., in S_8) doubly degenerate state of *e* symmetry in point group D_{2d} (the four-node ring-quantized orbital). In Gleiter's study, when the S_4N_4 molecule was artifically constrained to a planar D_{4h} geometry or to the S_8 puckered-ring geometry (D_{4d}), the ground state was a triplet configuration with a half-filled doubly degenerate orbital as the highest occupied MO. Thus, a Jahn-Teller distortion occurs to remove the degeneracy and results in the singlet ground-state configuration,[6] of Fig. 4 with symmetry D_{2d}.

Precisely the same effect occurs in our treatment when the S_8 geometry is used for the S_4N_4 molecule, with the exception that the half-filled highest occupied MO is derived from the S(3*d*) virtual atomic orbitals. Since the bond angles in such artificial molecules are unnatural, it is not surprising that the S(3*d*) orbitals are called upon to account for them. This result, however, is strictly a consequence of the artificial constraint on the geometry. In the real molecule, the Jahn-Teller effect prevents this occurrence.

It is evident, therefore, that the Jahn-Teller effect probably accounts for nonequivalent bond lengths in the $(SN)_x$ chains,[48,49] which are simply neutral molecules. The Jahn-Teller distortion is expected to be small due to the length of the "molecules." Both our calculations (see Appendix) and others[9,19] predict the existence of a one half-filled π orbital for the highest occupied MO in SN molecules used as the basis states in $(SN)_x$ band structure calculations. The trends revealed in the present study indicate that the $(SN)_x$ molecules will tend to distort their geometry in such a fashion as to remove the tendency for a half-filled highest occupied MO. The weak S-S interchain interaction, discussed above, may then become the more important issue in determining the details of the conduction and valence bands in a proper three-dimensional treatment of the $(SN)_x$ crystal.

The third important aspect of the frontier orbitals lies in their contributions to the uv absorption spectrum. All of the low-energy "optical" transitions (in the range $2.6 \lesssim h\nu \lesssim 6$ eV for S_4N_4: see Fig. 5) occur via the creation of particle-hole eigenstates which are linear combinations of these one-electron orbitals. Comparing Fig. 5 with Table III reveals that, as expected for such molecules,[21,22,23] the lower-energy optical transitions occur at roughly half the energy of the difference between the energies of the lowest empty and highest filled one-electron orbital eigenstates. This result is indicative of strong molecular exciton binding, and suggestive of a highly electric-field-dependent photogeneration in solid S_4N_4. Moreover, it is evident from Figs. 5 and 7 that the consequences of configuration interaction are quite large, thereby invalidating the simple one-electron models of the optical spectrum which heretofore have dominated the literature on this topic.[2-5]

TABLE V. CNDO-S eigenvalues spectrum of S_2N_2.

Orbital	Symmetry	Energy (eV)
Virtual		
12	$2b_{1u}$	−3.94
Occupied		
11	$1b_{3g}$	−11.01
10	$1b_{2g}$	−11.49
9	$2b_{3u}$	−11.85
8	$2b_{2u}$	−11.95
7	$1b_{1g}$	−13.65
6	$1b_{1u}$	−13.80
5	$3a_g$	−13.86
4	$2a_g$	−19.72
3	$1b_{2u}$	−19.84
2	$1b_{3u}$	−27.69
1	$1a_g$	−31.51

Finally, we come to the issue of electron delocalization. While we have not attempted to construct localized orbitals from our CNDO-S eigenstates, it is evident from Fig. 7 that the character of the upper p-derived orbitals does not lend itself to the construction of states localized on the N atoms. In particular, only one orbital ($2a_2$) is available for formation of (eight) N "lone-pair" localized p orbitals. Moreover, the strong but asymmetric S-N mixing seems to be associated with the large difference in I_p between the sulfur and nitrogen which, in turn, leads to the large charge transfer ($q \approx \frac{1}{2}e$). Thus, we infer that the doubly coordinated nitrogen atoms in S_4N_4, S_2N_2, and $(SN)_x$ are associated with delocalized frontier orbitals and with substantial charge transfer, both driven by the fact that $I_p(N) - I_p(S) = 2.3$ eV is large and positive. This conclusion in turn suggests that whereas $(SeN)_x$ and $(TeN)_x$ may exist in linear chain polymeric form, polymers of the form $(SP)_x$, $(SeP)_x$, $(TeP)_x$, $(SAs)_x$, $(SeAs)_x$, $(TeAs)_x$, etc, are rather unlikely to occur because the comparable I_p values of S, Se, Te, P, and As leads to cagelike molecular solids in which the group-V atom is triply rather than doubly coordinated.

TABLE VI. CNDO-S eigenvalue spectrum of "SN".

Orbital	Energy (eV)
Virtual	
8	−1.17
7	−5.47
Occupied	
6	−5.47
5,4	−12.27
3	−13.04
2	−20.36
1	−28.42

V. SUMMARY

The photoemission spectra of S_4N_4 molecules have been measured and analyzed using a self-consistent molecular-orbital model. The x-ray photoemission spectra of the N(1s) and S(2p) core levels, when compared with those of charge neutral atoms in N_2 and S_8 molecules, respectively, indicate an effective charge transfer of about one-half of an electronic charge from the sulfur atoms to the nitrogen atoms. By observing the cutoff energy of the true secondary electrons, the core-level spectra on solid samples has been compared directly to those in the vapor phase. From these measurements, a polarization energy of about 1.2 eV is deduced. The uv photoemission spectra of S_4N_4 molecules in the vapor provides a measure of the upper filled and lower empty one-electron energy levels. Our CNDO-S model, fit to the UPS gas-phase data, accurately produces both the XPS valence-band density of states, and,

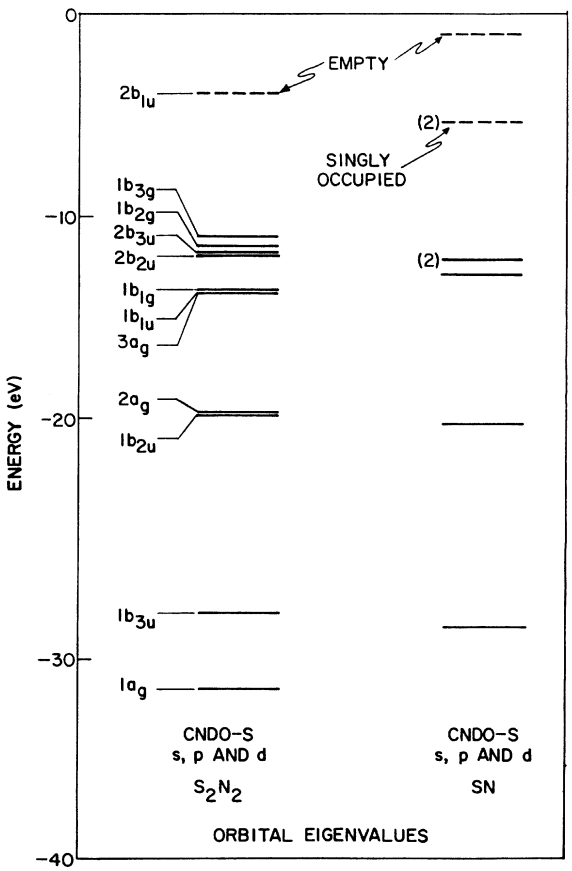

FIG. 8. Diagrammatic indication of the CNDO-S orbitals for S_2N_2 and "SN."

through the use of a configuration-interaction treatment of CNDO-S eigenstates, *also* describes the first few optical transitions of S_4N_4 molecules in solution. The optical spectra are dominated by molecular excitons, since the first optical transition is approximately half of the one-electron band gap.

The MO's nearest the Fermi level (the highest occupied and the lowest unoccupied MO) are shown to correspond almost entirely to the weak S-S bond across the plane of the four nitrogen atoms. This result suggests that weak S-S interchain interactions between $(SN)_x$ molecules may play a significant role in determining the band structure of $(SN)_x$ crystals. Finally, a case for nonequivalent bond lengths in $(SN)_x$ chains is presented in terms of a Jahn-Teller distortion, and it is inferred that structures analogous to $(SN)_x$ are unlikely to occur if N is replaced by a heavier group-V element.

ACKNOWLEDGMENTS

The authors are indebted to Professor D. T. Clark of the University of Durham, U. K., for providing the original version of our CNDO-S MO computer program, to Dr. N. O. Lipari, Dr. P. Nielson, and Dr. J. Ritsko of the Xerox Research Laboratories, Professor J. Joannopoulos of M. I. T., and Professor Clark for stimulating and helpful discussions; to Dr. R. P. Messmer for communicating to us his results prior to publication; to Professor A. F. Garito for numerous preprints and the communication of structural information on $(SN)_x$; and to L. Kennedy for her assistance.

APPENDIX

This appendix contains the results of our model calculations for S_2N_2 and the hypothetical "molecule" SN. The bond length of 1.616 Å for SN corresponds to that in S_4N_4. Structural parameters for S_2N_2 were obtained from average bond lengths in crystal structure data supplied by Garito.[50] The S-N distance is 1.654 Å and the S-N-S and N-S-N angles are 90.398° and 89.602°, respectively.

Table V contains the orbital eigenvalue spectrum of S_2N_2 together with the irreducible representations of the point group D_{2h}. The numbering of these levels begins with the first valence orbital. The uppermost orbital ($2b_{1u}$) is the lowest unoccupied orbital.

Table VI shows the results of a similar calculation for SN. The orbital at −5.47 is twofold degenerate and contains a single electron.

The results for both S_2N_2 and SN are displayed in Fig. 8 in a format analogous to that of Fig. 6.

[1] I. Lindqvist, J. Inorg. Nucl. Chem. 6, 159 (1958).
[2] D. Chapman and T. C. Waddington, Trans. Faraday Soc. 58, 1679 (1962).
[3] F. S. Braterman, J. Chem. Soc. 2297 (1965).
[4] A. G. Turner and F. S. Mortimer, Inorg. Chem. 5, 906 (1966).
[5] J. B. Mason, J. Chem. Soc. A, 1567 (1969).
[6] R. Gleiter, J. Chem. Soc. A, 3174 (1970).
[7] P. Cassoux, J. F. Labarre, O. Glemser, and W. Koch, J. Mol. Struct. 13, 405 (1972).
[8] M. S. Gopinathan and M. A. Whitehead, Can. J. Chem. 53, 1343 (1974).
[9] D. R. Salahub and R. P. Messmer, J. Chem. Phys. (to be published).
[10] B. D. Sharma and J. Donohue, Acta Crystallogr. 16, 891 (1963).
[11] F. Jellnick, in *Inorganic Sulfur Chemistry*, edited by G. Nickless (Elsevier, Amsterdam, 1968), Chap. 19.
[12] P. L. Kromick, H. Kaye, E. F. Chapman, S. B. Mainthia, and M. M. Labes, J. Chem. Phys. 36, 2235 (1962).
[13] V. V. Walatka, Jr., M. M. Labes, and J. H. Perlstein, Phys. Rev. Lett. 31, 1139 (1973).
[14] C. Hsu and M. M. Labes, J. Chem. Phys. 61, 4640 (1974).
[15] R. L. Greene, P. M. Grant, and G. B. Street, Phys. Rev. Lett. 34, 89 (1975); and R. L. Greene, G. B. Street, and L. J. Suter, Phys. Rev. Lett. 34, 577 (1975).
[16] A. A. Bright, M. J. Cohen, A. F. Garito, A. J. Heeger, C. M. Mikulski, P. J. Russo, and A. G. Mac Diarmid, Phys. Rev. Lett. 34, 206 (1975).
[17] H. Kamimura, A. J. Grant, F. Levy and A. D. Yoffe, Solid State Commun. 17, 49 (1975).
[18] M. Schlüter, J. R. Chelikowsky, and M. L. Cohen, Phys. Rev. Lett. 35, 869 (1975).
[19] A. A. Bright and F. Soven, Solid State Commun. (to be published).
[20] W. R. Salameck, K. S. Liang, A. Paton, and N. O. Lipari, Phys. Rev. B 12, 725 (1975).
[21] W. R. Salaneck, N. O. Lipari, A. Paton, R. Zallen, and K. S. Liang, Phys. Rev. B 12, 1493 (1975).
[22] C. B. Duke, N. O. Lipari, W. R. Salaneck, and L. B. Schein, J. Chem. Phys. 63, 1758 (1975).
[23] J. A. Pople and D. L. Beveridge, *Approximate Molecular Orbital Theory* (McGraw-Hill, New York, 1970).
[24] J. N. Murrell and A. J. Harget, *Semi-Empirical Self-Consistent Field Molecular Orbital Theory of Molecules* (Wiley-Interscience, London, 1972).
[25] M. B. Goehring, *Inorganic Syntheses* (McGraw-Hill, New York, 1960), Vol. 6, p. 123.
[26] M. V. Blanco and W. L. Jolly, *Inorganic Syntheses*, Vol. 9, (McGraw-Hill, New York, 1967), Vol. 9, p. 88.
[27] E. R. Lipincott and M. C. Tobin, J. Chem. Phys. 21, 1559 (1953).
[28] J. H. Scofield, J. Electron Spectrosc. (to be published).
[29] D. L. Ames, J. P. Maier, F. Watt, and D. W. Turner, J. Chem. Soc. Faraday Disc. 54, 277 (1972).
[30] G. Johansson, J. Gedman, A. Berndtsson, M. Klasson, and R. Nilsson, J. Electron. Spectrosc. 2, 295 (1973).

[31]See, e.g., D. T. Clark, in *Electron Emission Spectroscopy*, edited by W. Dekeyser, L. Fiermans, G. Vanderkelen, and J. Vennik (Reidel, Dordrecht, 1973), Chap. 6.
[32]S. Evans, Chem. Phys. Lett. 23, 134 (1973).
[33]N. O. Lipari and C. B. Duke, J. Chem. Phys. 63, 1748 (1975); 63, 1767 (1975).
[34]M. Wolfsberg and L. Helmholz, J. Chem. Phys. 20, 837 (1952).
[35]J. M. Sichel and M. A. Whitehead, Theor. Chim. Acta 7, 32 (1967).
[36]M. J. S. Dewar and D. H. Lo, J. Am. Chem. Soc. 94, 5296 (1972).
[37]D. T. Clark, Tetrahedron 24, 2663 (1968).
[38]D. A. Lowitz, J. Chem. Phys. 46, 4698 (1967).
[39]C. R. Brundle, M. B. Robin, and H. Basch, J. Chem. Phys. 53, 2196 (1970).
[40]T. Koopmans, Physica 1, 104 (1933).
[41]C. B. Duke and W. R. Salaneck, Bull. Am. Phys. Soc. 21, 228 (1976).
[42]See, e.g., W. J. Geary, in *Inorganic Sulfur Chemistry*, edited by G. Nickless (Elsevier, Amsterdam, 1968), Chap. 3.
[43]R. J. Boyd and M. A. Whitehead, J. Chem. Soc. 73, 78, 81 (1972).
[44]See a synopsis by J. D. Joannopoulos and M. Kastner, Solid State Commun. 17, 221 (1975).
[45]See, e.g., R. S. Knox, *Theory of Excitons* (Academic, New York, 1963).
[46]K. Siegbahn *et al.*, Nova. Acta. R. Soc. Sci. Ups. IV, 20 (1967).
[47]W. I. Friesen, A. J. Berlinsky, B. Bergerson, L. Weiler and T. M. Rice, Bull. Am. Phys. Soc. 20, 360 (1975).
[48]A. G. MacDiarmid, C. H. Mikulski, P. J. Russo, M. S. Saran, A. F. Garito, and A. J. Heeger, J. Chem. Soc. Chem. Commun. 476 (1975).
[49]M. Boudeulle, Ph. D. thesis (University of Lyon, 1974); Cryst. Struct. Commun. 4, 9 (1975).
[50]A. F. Garito (private communication).